Macgregor, K., MacKinnon, G., Farmer, J. G., and Graham, M. C. (2015) Mobility of antimony, arsenic and lead at a former mine, Glendinning, Scotland. Science of the Total Environment, 529, pp. 213-222.

There may be differences between this version and the published version. You are advised to consult the publisher's version if you wish to cite from it.

http://eprints.gla.ac.uk/105736/

Deposited on: 22 January 2016

Mobility of antimony, arsenic and lead at a former antimony mine, Glendinning, Scotland

Kenneth Macgregor [a], Gillian MacKinnon [b], John G. Farmer [a], Margaret C. Graham [a]

[a] School of GeoSciences, University of Edinburgh, Crew Building, Alexander Crum Brown Road, Edinburgh EH9 3FF, United Kingdom

[b] Scottish Universities Environmental Research Centre, Scottish Enterprise Park, East Kilbride, Glasgow G75 0QF, United Kingdom

HIGHLIGHTS

• Solid phase speciation of antimony, arsenic, lead and iron differed between sites.

• Elevated soil porewater antimony concentrations were linked to DOM and spoil leaching.

• Leaching from spoil resulted in elevated antimony concentrations in stream water.

Abstract

Elevated concentrations of antimony (Sb), arsenic (As) and lead (Pb) in upland organic-rich soils have resulted from past Sb mining activities at Glendinning, southern Scotland. Transfer of these elements into soil porewaters was linked to the production and leaching of dissolved organic matter and to leaching of spoil material. Sb was predominantly present in truly dissolved (<3 kDa) forms whilst As and Pb were more commonly associated with large Fe-rich/organic colloids. The distinctive porewater behaviour of Sb accounts for its loss from deeper sections of certain cores and its transport over greater distances down steeper sections of the catchment. Although Sb and As concentrations decreased with increasing distance down a steep gully from the main spoil heap, elevated concentrations (~6-8 and 13-20 $\mu g\ L^{-1}$, respectively) were detected in receiving stream waters. Thus, only partial attenuation occurs in steeply sloping sections of mining-impacted upland organic-rich soils and so spoil-derived contamination of surface waters may continue over time periods of decades to centuries.

Capsule abstract: Production and leaching of dissolved organic matter led to the concomitant transfer of truly dissolved Sb to soil porewaters. Leaching of spoil-derived Sb impacted on the quality of receiving stream waters.

Keywords: Antimony, Humic substances, Colloids, Iron (oxy)hydroxides

1. Introduction

The marked rise in global antimony (Sb) production, e.g. from 55 kt in 1990 to 180 kt in 2012 (Butterman and Carlin, 2004; USGS, 2013), is largely attributable to its use in flame retardants, car brake liner lubricants, catalysts for the production of polyethylene terephthalate (PET) and alloy additives (Filella *et al.,* 2002a; Ceriotti and Amarasiriwardena, 2009; Bach *et al.*, 2012; USGS, 2013). Currently, ~84% of global Sb production takes place in China (He *et al.*, 2012) and, although some large-scale mines have recently closed (USGS, 2013), many are operational, e.g. at the Dachang and Zhazaixi deposits in Guangxi and Hunan provinces, respectively. Significant environmental and human health impacts are associated with on-going ore extraction and smelting processes but there are also environmental concerns relating to historical sites. In the UK, Sb mining and smelting activities ceased in the mid-20th century (Flynn *et al.*, 2003) but impacts upon soils and waters are still observed in the 21st century (Flynn *et al.*, 2003; Gál *et al.,* 2007). In addition, Sb mining and smelting processes usually release arsenic (As) and lead (Pb) to the environment since all three elements commonly co-occur in the sulfidic ore deposits. In Europe, Sb is a list II pollution reduction substance

(EC, 2001), with some chemical forms considered to be carcinogenic (IARC, 1989). Arsenic is similarly classified whilst Pb is a list I priority hazardous substance by the EU Water Framework Directive (EC, 2000).

This study focuses on the Glendinning mine located in Dumfries and Galloway, SW Scotland (Fig. 1(a)–(b)), from which ~200 t of Sb ores were extracted during three main production periods, 1793–1798, 1888–1891 and 1919–1922 (Gallagher *et al.*, 1983). Ore smelting took place at Jamestown, ~1 km downhill of the mine (Gallagher *et al.*, 1983). Several spoil heaps in the vicinity of the mine are still evident, and previous studies have reported Sb concentrations of 14.0–673 mg kg^{-1} (Flynn *et al.*, 2003) and 10.3–1200 mg kg^{-1} (Gál *et al.*, 2007) in the surrounding soils. Whilst these studies demonstrated that the soil Sb concentrations were significantly elevated above background levels, the geochemical associations, lateral and vertical elemental mobility and transport mechanisms for Sb, As and Pb at the site remain poorly defined. The mobility of contaminants in soil is often influenced by key variables such as drainage, pH, redox status, organic matter content and the abundance of major elements such as iron (Fe) in the soil. Many of these factors are interlinked and, for example, drainage and pH are particularly important with respect to redox cycling of Fe. Iron oxides are major natural sorbents for Sb (Johnson *et al.*, 2005; Mitsunobu *et al.*, 2006, 2010; Wilson *et al.*, 2010; Okkenhaug *et al.*, 2011), and Filella *et al.* (2002b) noted the importance of Fe (oxy)hydroxides in limiting Sb mobility, particularly in acidic soils typical of those found at the Glendinning site. As in many upland areas of the UK, the soils are also organic-rich and previous work has shown that Sb, As and Pb bind to organic matter to varying extents (e.g. Buschmann and Sigg, 2004; Buschmann *et al.*, 2006). For example, several studies have shown significant binding of Sb to soil humic acids (Buschmann and Sigg, 2004), whilst others found only limited organic complexation within soils (Filella, 2011). Lead has been shown to be largely immobile in upland organic-rich soils in NE Scotland but during storm events it can be released in association with organic-rich colloids (Graham *et al.*, 2006). A recent study also showed that phase associations of Pb were influenced by soil pH with significant adsorption to organic matter at pH <5 but preferential adsorption to Fe (oxy)hydroxides at higher pH (Shi *et al.*, 2013). Iron (oxy)hydroxides also act as a control on As mobility due to the high affinity of As for these phases under oxic conditions. Some studies, however, have shown that these interactions can be modified and sometimes enhanced by the presence of natural organic matter (NOM) (e.g. Redman *et al.*, 2002). Subtle differences in associations, e.g. direct binding to Fe oxides vs bridging between NOM and Fe oxides vs direct binding to NOM, are important because they may influence the form in which such elements are released into soil porewaters and their subsequent fate (e.g. Neubauer *et al.*, 2013).

This study determines the concentrations and associations of Sb, As and Pb in soil, porewater, surface flow and stream waters in order to assess elemental mobility and transport processes operating in the vicinity of a large spoil heap at the abandoned Glendinning Sb mine in Scotland.

2. Materials and methods

2.1. Sample collection

To demonstrate connectivity between spoil heap 1 (SpH1) and the receiving water, the Glenshanna Burn, 250 mL water samples were collected in pre-cleaned polyethylene bottles from surface flows in the small gully leading steeply down from SpH1 towards the Burn and directly from the Burn itself. In February 2013, stream waters W1 and W2 were collected upstream whilst W3 was collected downstream of SpH1. The two surface flows collected at the same time were designated W4 and W5 (Fig. 1(c)). Sampling was repeated in October 2014 at W1, W3, W4 and W5. Composite surface (0–5 cm; SpH1-surface) and subsurface (30–35 cm; SpH1-deep) spoil samples collected in February 2013 were stored in labelled polyethylene bags. Depending upon soil depth, ≤12 cm-deep cores also collected in February 2013 were taken using a spade and also placed in labelled polyethylene bags. These were collected at: (i) three locations (S1–3) along a 30-m transect from spoil heap 2 (SpH2) which was near the mine entrance towards a path; (ii) three locations (S4–6) along a 50-m transect down-gully from SpH1 towards the Glenshanna Burn; and (iii) a control site (C1) approximately 500 m further up the Glenshanna valley (Fig. 1). Soil core dimensions were ~20 cm × 20 cm × ~12 cm

depth and each core was sliced into 2-cm depth sections. Each section was weighed, air dried (25 °C; ~20 days), reweighed, sieved to <2 mm and ground using a mortar and pestle until a fine homogenised powder was achieved.
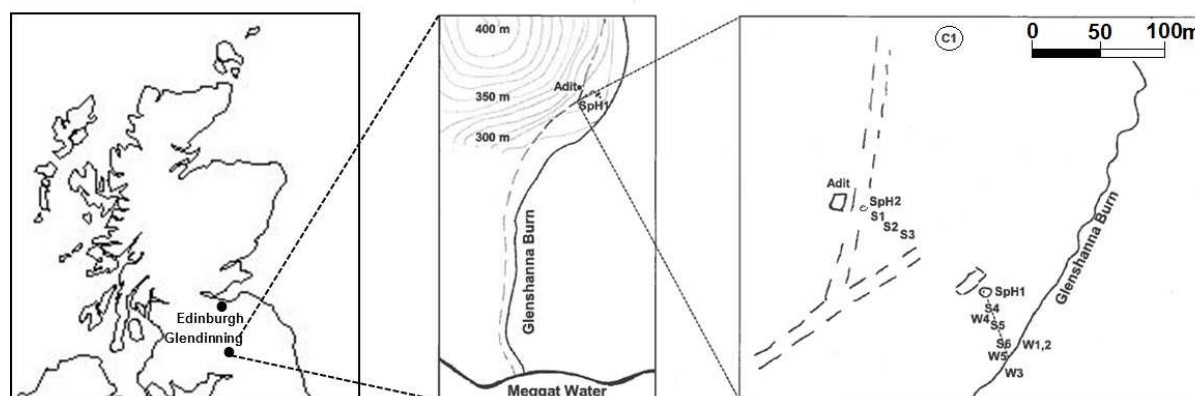
Fig. 1. (a) Map of Scotland showing the location of Glendinning; (b) schematic of the Glendinning mining site showing the location of the adit and main spoil heap (SpH1); and (c) enlarged schematic showing the location of soil and water sampling sites in relation to the adit and SpH1.

2.2. Sample preparation

2.2.1. Stream and surface flow water

Sub-samples (200 mL) of the stream water samples were acidified with 100 μL c.HNO$_3$ (Aristar, VWR International Ltd., Leics., UK), filtered through 1 μm membranes (Whatman cellulose nitrate membrane filter paper; VWR International Ltd., Leics., UK) and slowly concentrated tenfold on a hotplate. Reagent blanks were similarly prepared. The surface flow waters did not require pre concentration.

2.2.2. Soil samples

Soil pH was determined in soil suspensions (2.5 g soil in 12.5 mL 0.01 M CaCl$_2$) using a calibrated pH meter (Jenway model 3505). Approximately 0.25 g of each soil section was oven-dried (105 °C; 12 h). The organic matter (OM) content was determined relative to the oven-dried mass after ashing (450 °C; 4 h). The ash residue was digested using a MARS 6 microwave digestion system (CEM) and the modified US EPA Method 3052 (HF–HNO$_3$ Aristar, VWR International Ltd., Leics., UK) published by Yafa and Farmer (2006). With every batch of ten samples, duplicate reagent blanks and duplicate samples of a peat certified reference material (NIMT/UOE/FM001 (Yafa *et al.,* 2004)) were taken through the same procedure (see SI file).

2.2.3. Porewater extraction and ultrafiltration

In accordance with the method in Graham *et al.* (2008), porewaters were isolated by centrifuging fresh soil at 8873 ×g for 10 min. The supernatant was filtered through 0.2 μm (Whatman, hydrophilic) membranes. For S2–5 porewaters, the UV absorbance at 252 nm was used as a proxy for dissolved organic matter (DOM) concentration (Graham *et al.,* 2008). A 20 mL subsample of the 0.2 μm-filtrate was then ultracentrifuged (3 kDa Vivaspin 20; polyethersulfone membranes; VWR International Ltd., Leics., UK) at 6655 ×g (60 min). The ultra-filtrate (truly dissolved fraction) and ultrafilter retentate (colloidal fraction) were quantitatively removed and stored in separate sterilin tubes ready for

measurement of UV absorbance at 252 nm (Unicam UV2 spectrometer) and elemental analysis (see Analysis section below).

2.2.4. Sequential extraction

The three-stage BCR sequential extraction detailed by Davidson *et al.*(1998) was followed (see SI file). In brief, BCR1, 2 and 3 remove the exchangeable/acid-soluble, reducible (e.g. Fe/Mn (oxy)hydroxide) and oxidisable (e.g. organic matter, sulfide) phases, respectively, from the soil whilst the residual fraction comprises non-extractable phases.

2.2.5. Gel electrophoresis

The ultrafiltration retentate (3 kDa–0.2 μm) from selected soil porewaters underwent gel electrophoretic fractionation (Fisherbrand horizontal miniplus unit) as described in Graham *et al.* (2008).

2.3. Analysis

Concentrations of Sb (206.836 nm), As (228.812 nm), Pb (220.353 nm) and Fe (239.562 nm) in soil digests were determined by Inductively Coupled Plasma-Optical Emission Spectroscopy (ICP-OES) using a Perkin–Elmer Optima 5300DV instrument (Perkin–Elmer, Beaconsfield, UK). Calibration standards (0.01–300 mg L−1) were prepared using a 1000 mg L^{-1} ICP standard solution (in 1 M HNO_3; Fisher Scientific) for Sb, and an ICP Multielement Standard Solution IV CentiPUR (Merck) for As, Pb and Fe. Calibration curves for both low and high-concentration samples were obtained. Analytical precision (±RSD) for the independent reference solution, ICP Multielement Standard Solution VI (Pb: 10 mg L^{-1}; As and Fe: 100 mg L^{-1}), was <3.3% (n = 10). Analysis of ombrotrophic peat reference material NIMT/UOE/FM001 (Yafa *et al.,* 2004) gave concentrations (Sb 2.00 ± 0.43, As 3.00 ± 0.56, Pb 159 ± 6 and Fe 803 ± 46, all in mg kg^{-1}; n = 12) which were in good agreement with the certified (Pb 174 ±8 mg kg^{-1}), and information only values (As 2.44 ± 0.55; Sb 2.37 ± 0.34; Fe 921 ± 84 mg kg^{-1}) (Yafa *et al*., 2004; Cloy *et al.,* 2009).

Elemental (Sb, As, Pb and Fe) concentrations in stream water, surface flow, porewater and gel electrophoresis samples were determined by Inductively Coupled Plasma-Mass Spectrometry (ICP-MS) using an Agilent 7500ce instrument (Agilent Technologies, Stockport, UK) with nickel cones. Calibration standards (0.01–1000 μg L^{-1}) and curves for both low- and high-elemental concentrations were prepared. Analysis of the National Institute of Standards and Technology (NIST) Standard Reference Material (SRM) 1640 Trace Elements in Water gave values of Sb 58.2 ± 2.9 μg L^{-1}, As 58.3 ± 1.6 μg L^{-1}, Pb 21.9 ± 2.6 μg L^{-1} and Fe 100.1 ± 5.0 μg L^{-1} (n = 5) which compared well with the certified values (Sb 58.3, As 64.3, Pb 19.6 and Fe 98.1 μg L^{-1}).

3. Results

3.1. Soil pH, OM content and elemental (Fe, Sb, As and Pb) concentrations in soil and soil porewaters

3.1.1. Soil pH

There was typically little variation in soil pH with increasing depth. The lowest pH values (3.9–4.1) were obtained for the control soil (C1) but low pH values were also obtained for S4 (4.7–4.9) and S1 (4.4–5.2), i.e. those closest to the spoil heaps, SpH1 and SpH2, respectively. The pH values for the soils at S2, S3, S5 and S6 were slightly less acidic and ranged from 5.4–6.3 (Table 1).

3.1.2. OM content

The OM content for C1 soils was in the range of ~15–95% w/w and highest in the top 0–5 cm sections. The exceptionally high OM content, especially in the top sections (SI file), may account for the low pH of the control soil. With the exception of S2 which had a maximum value of ~77%, peak OM content for S1–6 soils was typically ~39–54% w/w (Table 1). The vertical OM profiles for S1–6 all showed similar trends, decreasing from the surface towards the bottom of the cores (Fig. 2), and were consistent with the soil type for the area which comprises a peaty layer overlying silty-clay mineral soils (Gallagher *et al.,* 1983). The porewaters extracted from the soils were pale brown-coloured, indicating the presence of dissolved humic substances. With the exception of S5, where absorbance values at 252 nm (a measure of colour) remained approximately constant, the maximum absorbance occurred at depths of 5–8 cm in each core. This was ~5 cm below the maximum solid phase OM content (Fig. 2), similar to results observed in many other studies (e.g. Michalzik and Matzner, 1999). The DOM profile shape is the result of production and leaching in the upper layers and removal via adsorption in the deeper layers (Kalbitz *et al.*, 2000; Kalbitz and Kaiser, 2008).

3.2. Iron

The Fe concentrations in the control soil core C1 were ~0.1–3.4% w/w (Table 1) whilst those for S1–6 were in the range of ~0.2–6.3% w/w (Fig. 2), with highest values occurring in the soils closest to SpH1 and SpH2. In contrast with OM content, the vertical profiles for Fe showed very low concentrations in the top sections and then a general trend of increasing concentration with increasing depth, reflecting the transition from the peaty surface layer to mineral-rich material. Porewater Fe concentrations were also typically greater at depth than at the surface but there was no strong relationship with solid phase Fe concentration. Consistent with a transition to reducing conditions, for S2, S4 and S5 there was a clear subsurface maximum at ~5–10 cm and, for S3, the Fe concentration continued to increase to the bottom of the core. Highest porewater concentrations of ~80 mg L^{-1} were obtained for the deeper sections of S3 and S5.

3.3. Antimony

The mean and range of Sb concentrations in soils from C1 were 0.7 ± 0.3 mg kg^{-1} and 0.4–1.2 mg kg^{-1} (Table 1), respectively, consistent with the values of 0.6–1.05 mg kg^{-1} for local soils obtained as part of the FOREGS study (Salminen *et al*., 2005) and indicative of no influence from the nearby mining activities. In contrast, concentrations in S1–6 soils were several orders of magnitude higher. Maximum values of ~260 mg kg^{-1} were found in S3 soils and, for S4–6, there was a clear trend of decreasing concentration with increasing distance downslope from SpH1 (Fig. 2). The porewater Sb concentrations for S4 and S5 also reflected this trend with distance from SpH1 (Fig. 2).

Regression analysis showed that there was a strong relationship between solid phase OM content and Sb concentrations at S3 ($P < 0.01$, $R^2 = 0.95$). Although the porewater Sb and solid phase Sb profiles for S2–5 appeared to be unrelated, there were strong correlations between the porewater concentration profiles of Sb and DOM (e.g. S3: $P < 0.01$, $R^2 = 0.95$) and of Sb and Fe (e.g. S3: $P < 0.01$, $R^2 = 0.98$). An exception was S5, however, where the Sb porewater profile was distinctly different from those of both Fe and DOM (Fig. 2).

Table 1: Elemental concentration range found in control soil (C1), spoil (SpH1), soil profile (S1-6) and water (W1-5) samples taken in the vicinity of Glendinning antimony mine

Samples collected	pH	%OM	Fe %	Sb mg kg^{-1}	As mg kg^{-1}	Pb mg kg^{-1}
C1	3.9 – 4.1	14.8 – 95.3	0.11 – 3.35	0.41 – 1.18	0.43 – 0.91	3.07 – 57.1
SpH1-surface[†]	5.0	7.31 – 10.9	3.98 – 5.26	174 – 302	74.0 – 85.0	873 – 1020
SpH1-deep[†]	6.6	2.82 – 3.77	4.02 – 4.46	300 – 541	104 – 170	421 – 621
S1	4.4 – 5.2	6.60 – 38.6	3.83 – 5.80	55.4 – 132	34.9 – 57.2	390 – 486
S2	6.0 – 6.3	21.0 – 77.2	0.21 – 4.86	95.5 – 222	5.68 – 55.6	91.6 – 710
S3	5.4 – 5.6	14.3 – 44.9	2.45 – 5.48	50.7 – 261	13.9 – 19.1	90.9 – 114
S4	4.7 – 4.9	23.2 – 53.6	2.51 – 6.28	120 – 188	18.4 – 75.3	52.2 – 632
S5	5.6 – 6.0	22.8 – 48.4	2.08 – 3.46	65.9 – 91.2	3.87 – 5.92	40.2 – 52.1
S6	5.7 – 6.0	13.0 – 44.6	1.94 – 4.50	6.77 – 21.7	0.36 – 1.40	27.9 – 88.6
Water sites			Fe µg L^{-1}	Sb µg L^{-1}	As µg L^{-1}	Pb µg L^{-1}
W1* 02/13			32.8 ± 0.04	0.10	1.13 ± 0.09	0.08 ± 0.03
10/14				0.26	0.89	0.38
W2*			32.0 ± 0.09	0.11	1.00 ± 0.01	0.08 ± 0.00
W3* 02/13			22.2 ± 3.79	5.88 ± 0.29	13.2 ± 1.14	0.07 ± 0.03
10/14				7.53	20.2	0.68
W4*			4.95 ± 2.69	83.8 ± 0.90	181 ± 26.4	0.55 ± 0.68
W5 02/13			5.31	783	1770	0.06
10/14				674	1480	0.21

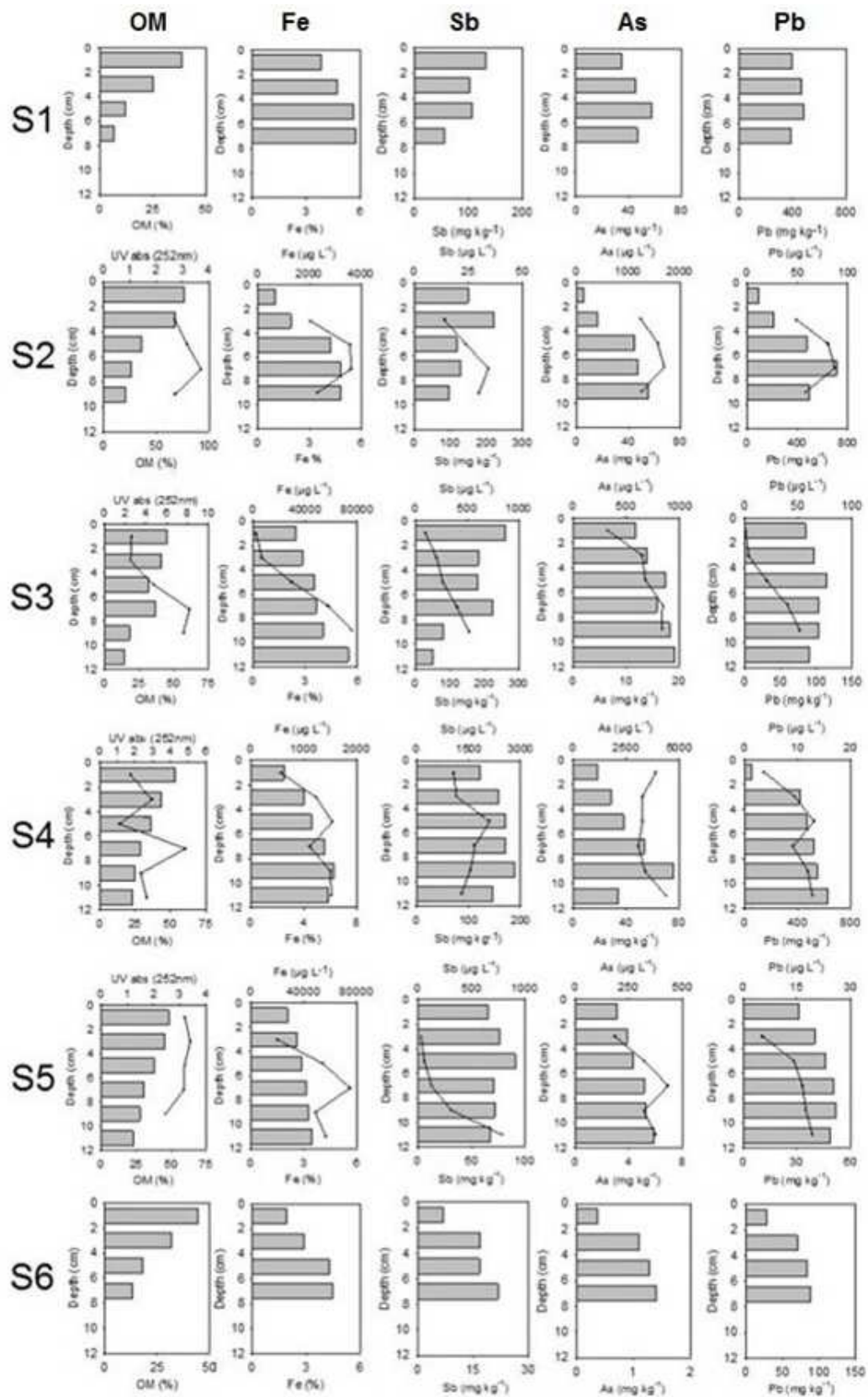[†] 6 sub-samples of spoil; * mean from duplicate analysis

Figure 2: Vertical variations in the concentrations of OM, Fe, Sb, As and Pb in solid phase soils (S1-6) and their respective porewaters (S2-5)

3.4. Arsenic

Arsenic concentrations of <1 mg kg^{-1} at C1 (Table 1) were again in good agreement with those reported in the FOREGS study for the locality (Salminen *et al*., 2005), similar to those in soils from S6 (<1.4 mg kg^{-1}) but at least an order of magnitude lower than those for S1–5. The highest As concentration of ~75 mg kg^{-1} was obtained at S4, the site closest to SpH1, and, as for Sb, As concentrations decreased with increasing distance downslope from SpH1. In agreement with the vertical Fe concentration profiles, however, As concentrations showed a general increase with increasing soil depth. For S2 and S5, there was also a strong relationship between porewater As and Fe concentrations, suggesting concomitant release from the soil solid phase.

3.5. Lead

In contrast with Sb and As, the C1 soil Pb concentrations were higher than expected based on its crustal abundance (~12–15 mg kg^{-1}) (Taylor, 1964; Wedepohl, 1995). Concentrations of up to 57 mg kg^{-1} were attributable to atmospheric deposition of Pb emissions from coal combustion, smelting and leaded gasoline in the industrial and post-industrial periods (Salminen *et al*., 2005; Cloy *et al.*, 2009; Farmer *et al*., 2010). However, considerably higher values (up to 710 mg kg^{-1}) were observed for S1–4, consistent with the additional contribution of mining-derived Pb to these soils, whilst those for S5–6 were similar to C1. The vertical concentration profiles for S1 and S3 had slight sub-surface maxima at ~5 cm depth whilst there was a general increase towards the bottom of each of the other cores. Highest concentrations of ~600–700 mg kg^{-1} were observed towards the bottom of S2 and S4. Akin to Sb and As, porewater Pb profiles bore little resemblance to the respective solid phase profiles; in the main, there was a strong similarity between the vertical porewater profiles of Pb and Fe.

3.6. OM content and elemental (Sb, As, Pb and Fe) concentrations in SpH1

As expected, the spoil samples had lower OM content than the surrounding soils (Table 1). There was, however, a thin coverage of soil like material supporting heathers and mosses and this was reflected in an OM content of ~7–11% w/w for SpH1-surface. With less soil present at depth, the OM content for SpH1-deep dropped to ~3–4% w/w. The ore material at Glendinning comprised stibnite (Sb2S3) and semseyite (Pb$_9$Sb$_8$S$_{21}$) in association with a stratiform arsenopyrite (FeAsS)–pyrite (FeS$_2$) mineralisation (Gallagher *et al*., 1983) and SpH1 samples contained elevated concentrations of Sb, As, Pb and Fe. The composition of the spoil was not uniform and the range of values reflects the analysis of six aliquots of these samples. Higher Sb and As concentrations of ~300–540 mg kg^{-1} and ~100–170 mg kg^{-1}, respectively, were obtained for SpH1-deep. In contrast, SpH1-surface had higher Pb concentrations of ~870–1020 mg kg^{-1}. The median Fe concentrations were 5.1% w/w and 4.2% w/w for SpH1-surface and SpH1-deep, respectively, and the range of Fe concentrations was also greater for the surface sample. The variation in composition may be attributable to changes in the nature of weathering processes operating at the surface and at greater depth within the spoil.

3.7. Stream water and surface flow elemental (Sb, As, Pb and Fe) concentrations

For samples collected in February 2013, aqueous phase Sb concentrations were ~0.1 μg L^{-1} at W1–2 (upstream of the gully) but ~5.9 ± 0.3 μg L^{-1} at W3 (downstream of the gully). Similar results of ~0.3 μg L^{-1} at W1 and 7.5 μg L^{-1} at W3 were obtained in October 2014, demonstrating that the waters flowing down the gully from SpH1 were transferring measurable Sb concentrations to the Glenshanna Burn. The W3 values were, however, ~ 100-fold lower than the values of ~780 μg L^{-1} (02/2013) and ~670 μg L^{-1} (10/2014) obtained at W5 (surface flow furthest down-gully from SpH1) (Table 1) and so considerable dilution had taken place upon entering the Burn. As for Sb, As concentrations were also lower at the upstream sites (~ 0.9–1.0 μg L^{-1}) than the values of ~13.2 ± 1.1 μg L^{-1} (02/2013) and 20.2 μg L^{-1} (10/2014) at the downstream site. Again, since the As concentrations at W5 were ~1770 μg L^{-1} (02/2013) and ~1480 μg L^{-1} (10/2014) the dilution upon entering the Burn was, to a first approximation, ~100-fold. Pb concentrations were generally low (0.06–0.08 μg L^{-1}) and there was no

difference between upstream and downstream waters nor was there any elevation in the surface flow, W5. Iron concentrations in stream waters W1–3 were higher than in W4–5 and, in contrast with the other elements, Fe concentration in the downstream sample, W3, was slightly lower than in the upstream samples (W1–2).

3.8. BCR sequential extraction of selected soil samples

Samples from 2–4 cm or 4–6 cm for each of S2–5 and from 6–8 cm and 8–10 cm for S2 and S4, respectively, were selected as exemplar near-surface and deeper sections (Fig. 3). Typical recoveries for Sb, As and Pb were ~80–100% whilst those for Fe were ~60%, the latter being attributable to the use of aqua regia rather than HNO3/HF for the digestion of the residual phase. The results for Sb showed that very little was extracted in BCR1 and 2 (<5% in total) from any of the samples. Approximately 66% was extracted in BCR3 from S2 2–4 cm which had ~70% w/w OM whilst ~15–20% was extracted from the other near surface samples which had ~45–55% OM. The two samples from the deeper sections of S2 and S4 had lower OM contents and <10% Sb was extracted in BCR3. For As, ~5–18% was extracted in BCR1 from the samples taken from S2 and S3 whilst <3% was found in the same fraction for samples from S4 and S5. About 3–24% was extracted in BCR2 with the greater proportions being extracted from the samples from the deeper sections of S2 and S4, and especially the S5 4–6 cm section. As for Sb, the greatest proportion of As (~65%) extracted in BCR3 was for the sample which had the highest OM content, S2 2–4 cm. The lowest proportions extracted in this fraction were again for the deeper sections of S2 and S4. In these samples and in S4 4–6 cm, the greatest proportion (60–~80%) of As was in the residual phase. For Pb, <1% was extracted in BCR1 and 2 from each of the samples. Approximately 65% Pb was in BCR3 for S2 2–4 cm whilst in all other samples, ~18–39% was extracted in this fraction. Thus the majority of Pb was present in the residual fraction in all samples except the highly organic S2 2–4 cm sample. For Fe the pattern was quite similar to that for Pb but with up to 12% in BCR2, 10–55% in BCR3 and the remainder in the residual phase. Although the overall extractability (sum of BCR 1–3) increased in the order Sb < Fe < Pb < As, the between-site and "with-depth" trends were quite similar for all four elements.

3.9. Elemental (Sb, As, Pb and Fe) concentrations in colloidal and dissolved fractions of the soil porewaters from S2–5

In general, the proportion in the colloidal fraction increased in the order Sb ≤ As ≤ Pb ≤ Fe (Fig. 4) but there were considerable variations with depth for both Sb and As. At S2, there was ~ 65–70% colloidal Sb in the near-surface porewaters which decreased to ~30% towards the bottom of the core. At S5, values ranged from 6–55% but at S3 and S4 there was <25% Sb in the colloidal fraction of the porewaters. The distribution of As between colloidal and truly dissolved forms was similar to Sb in the S4 porewaters but, for S2, S3 and S5 there were distinct differences, e.g. there was an increase from ~20% to ~80% As in the colloidal fraction of S3 porewaters with increasing depth whilst the amount of colloidal Sb remained <20%. Similar trends were evident for the S5 porewaters and it was clear that there were site-specific differences between the porewater distributions of Sb and As. With the exception of Pb in the porewaters of S3 and the bottom section of S5, both Pb and Fe were almost exclusively present in the colloidal fraction, These results are consistent with previously published work (e.g. Graham *et al*., 2006; Schroth *et al*., 2008) showing that Pb solubility is enhanced by association with both organic and Fe-rich colloids.

3.10. Gel electrophoretic patterns

For the 4–6 cm ultrafilter retentate from S2 and S5, the highest concentrations of Sb, As and Fe were found in the fractions closest to the gel well (Fig. 5 and SI file). Thus Sb and As were associated with large Fe rich humic colloids. In comparison, for the 4–6 cm samples from S3 and S4, Sb and As were associated with smaller organic colloids (SI file). The distribution of Pb was similar to that of Fe at S2

and S3 but, at both S4 and S5, Pb was predominantly associated with small organic colloids and there was little correlation between the distribution of Pb and those of Sb or Fe (Fig. 5 and SI file).

4. Discussion

4.1. Antimony and other elemental concentrations in the spoil heap (SpH1)

Antimony, As and Pb concentrations in the spoil material from SpH1 were typically higher than those in all six soil cores (S1–6) and the control soil (C1) (Table 1). Excavation of the lower mining area (Gallagher *et al*., 1983), which ran underground from the adit to a shaft near SpH1 (Fig. 1(b)–(c)), resulted in spoil with high mineral content (stibnite (Sb_2S_3), arsenopyrite (FeAsS) and galena (PbS)) being deposited on the surrounding land and this has subsequently been exposed to the atmosphere and subject to infiltration of rainwater. Biver and Shotyk (2012) studied the kinetics of Sb release from stibnite and showed that higher rates of dissolution occurred as pH decreased from 5.1 to 1.1 and also with increasing dissolved oxygen concentrations from 0.05 to 0.8 atm. The lower concentrations of antimony in the surface spoil are most likely a consequence of greater stibnite weathering rates in the surface spoil. Oxidative dissolution of arsenopyrite also releases As and Fe into solution but the latter tends to hydrolyse and precipitate in the form of Fe (oxy)hydroxides (e.g. Walker *et al*., 2006). Moreover, coatings on the surface of Sb-containing munitions have been shown to be enriched in both Fe and Pb (Ackerman *et al*., 2009). Thus at Glendinning, we propose that oxidative dissolution processes lead to the loss of Sb (Biver and Shotyk, 2012) and As (Walker *et al*., 2006) whilst precipitation favours the enrichment of Fe and Pb in surface spoil. At depth, reductive dissolution of Fe (oxy)hydroxides favours the loss of both Fe and Pb from surface coatings, accounting for the lower concentrations of these elements in SpH1-deep.

4.2. Processes controlling the spatial distribution and associations of Sb, As, Pb and Fe in soils at the Glendinning site

4.2.1. Down-slope from the adit

Core S1 was situated below SpH2 on a shallow slope leading down from the adit whilst S2–3 were in a water-logged area at the base of this slope (Fig. 1(b)–(c)). Antimony concentrations consistently decreased with increasing soil depth whilst the profiles for As, Pb and Fe showed either increased or near-constant concentrations with increasing depth. Based on the similarity of their vertical profiles, Sb may be strongly retained by OM in the near-surface sections of S1–3. This would be consistent with results for shooting range soils which attributed strong retention in surface organic layers to Sb(V) binding by humic acids (Steely *et al*., 2007).

The soil concentrations of Sb increased along the transect from S1 to S3 but this trend was not observed for As and Pb (Table 1 and Fig. 2). Thus, although originating from the same source material, the processes controlling not only vertical but also lateral mobility have affected Sb differently from As and Pb. There was little variation in pH with increasing soil depth (Table 1) nor was there an obvious relationship between pH and elemental concentration with distance downslope from SpH2. The profiles of As and Pb generally followed the trend for Fe at each of S1–3 and so sequential extraction was expected to reveal a major difference between the solid phase associations of Sb and those of As and Pb. In contrast with the anticipated results, all four elements behaved similarly. For example, the majority of each was associated with OM at S2 (2–4 cm) whilst at S3 (2–4 cm) the majority of Sb, Pb, Fe and ~50% As was in the residual phase. Comparison of the data for the 2–4 cm and 6–8 cm sections for the S2 core also revealed a consistent change for all four elements with increasing depth: the proportion associated with OM decreased markedly, resulting in a concomitant increase in the percentage present in the residual fraction (Fig. 3). Thus, solid phase associations per se do not explain the observed differences in vertical and lateral distribution of Sb in comparison with As and Pb (Fig. 2).
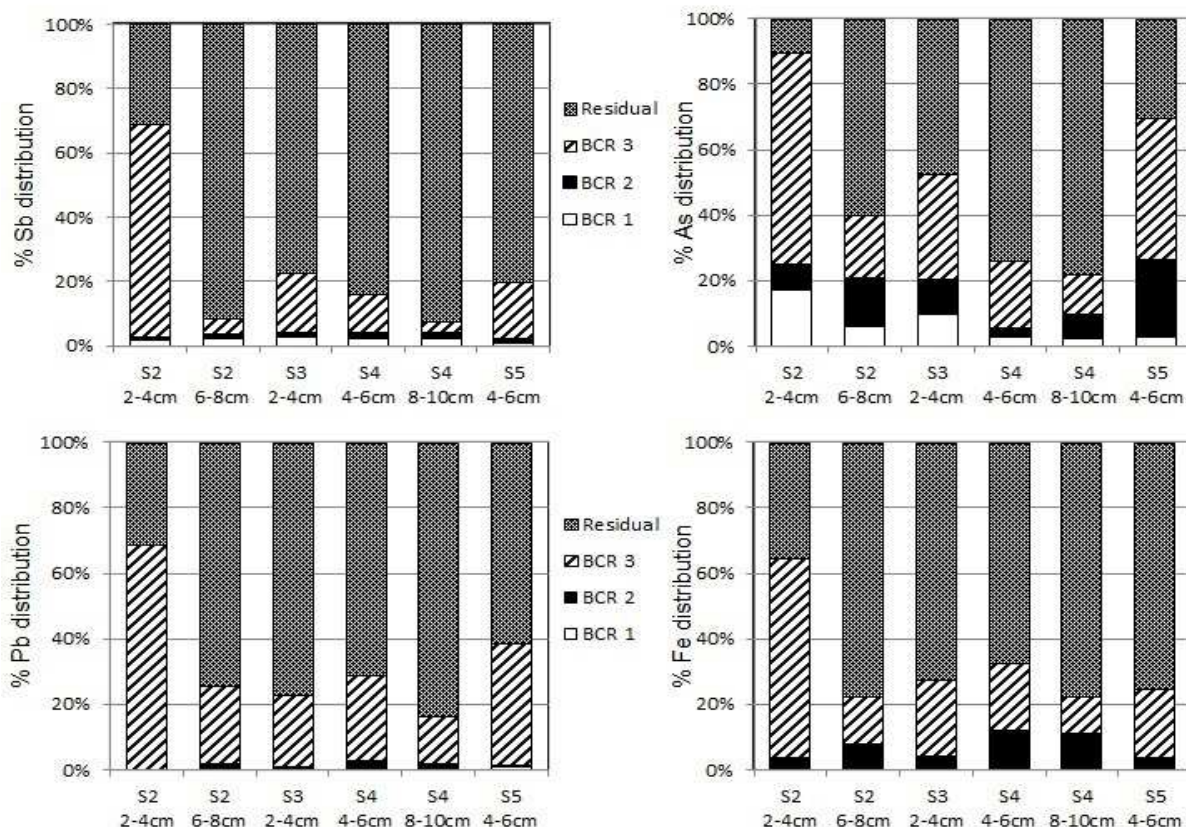
Fig. 3. Distribution of Sb, As, Pb and Fe amongst BCR fractions (exchangeable, reducible and oxidisable) and the residual phase of selected soil samples from S2–5.

A further confounding feature of the data was that at S2 and at S3 the porewater profiles for Sb, As and Pb were very similar to each other and, in each case, were similar to those of both DOM and Fe (Fig. 2). However, when the distribution between colloidal and truly dissolved forms was considered (Fig. 4), there was a significant difference between the distributions of Sb and As and those of Pb, Fe and DOM (colour strongly retained in the colloidal fraction; data not shown). For the latter group, the vast majority (70–100%) was present in the colloidal fraction whilst up to ~90% Sb and up to ~80% As were present in the truly dissolved fraction. Moreover, for S2, there was a major change from colloidal Sb in the near-surface sections to truly dissolved forms at depth whilst, at S3, the proportion in the truly dissolved phase remained almost constant with depth. At both locations, this strongly contrasted with the distribution of As: at S2, there was little change with depth whilst at S3, the proportion of colloidal As increased with increasing depth and thus the behaviour of As became more similar to that of Pb, Fe and OM. We propose that lateral transport promotes the removal of truly dissolved Sb species from these deeper sections of the soil whilst association of As and Pb with large Fe-rich/organic colloids favours their retention.

For S2 4–6 cm, where the solid phase associations indicated that large proportions of Sb, As, Pb and Fe were associated with organic matter, more than 50% of each element was in colloidal forms within the porewater. Gel electrophoresis confirmed a strong association of Sb, As and Pb with very large Fe-rich organic colloids which have low mobility. For S3 4–6 cm, where the solid phase association with organic matter was lower, Sb was mainly in the truly dissolved fraction and gel electrophoresis showed that, within the colloidal fraction, the greater proportion of As was again associated with very large Fe-rich colloids. Overall, the results of both ultrafiltration and gel electrophoresis point to differences in associations, which may start to explain the differences in the vertical distribution of Sb compared with As, Pb and Fe.
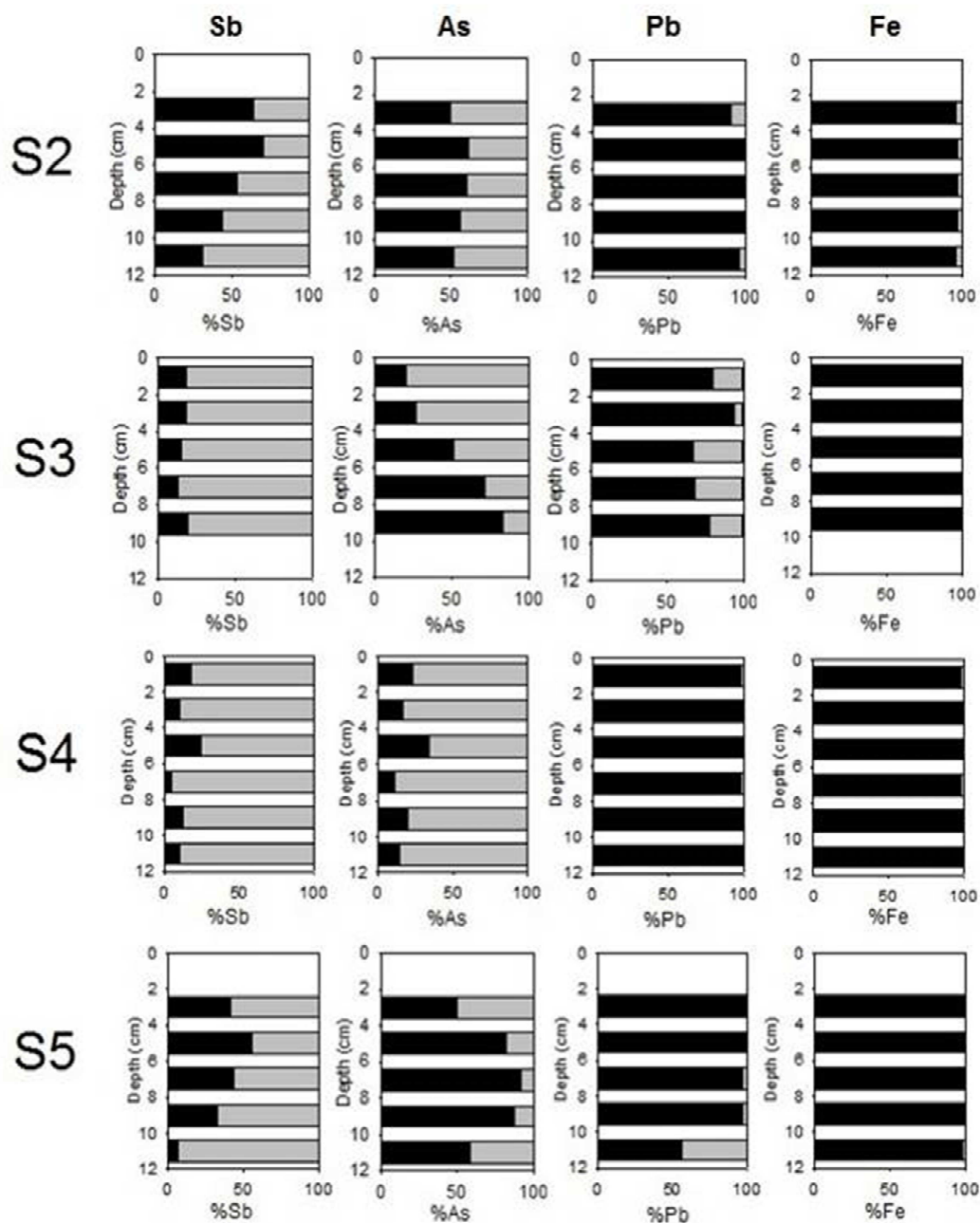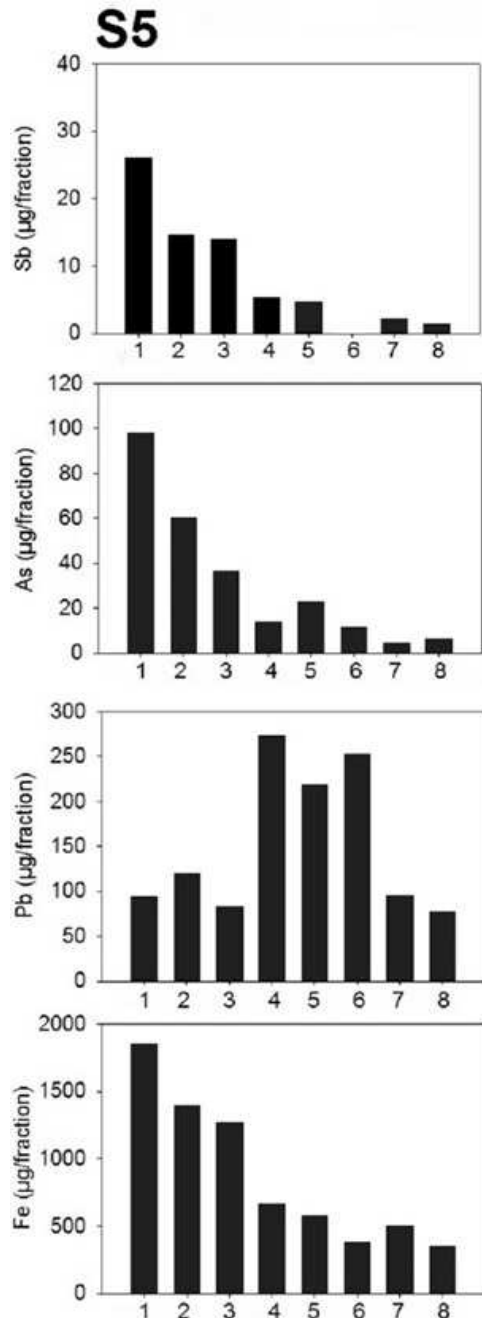
Fig. 4. Vertical variations in the distribution of Sb, As, Pb and Fe amongst colloidal (3 kDa–0.2 μm) and dissolved fractions (<3 kDa) of the porewaters from S2–5. Colloidal fraction in the black: dissolved fraction in light grey.

4.2.2. Down-gully from SpH1

There were ~2-fold and ~9-fold decreases in the maximum Sb concentration in the solid phase soils between S4 and S5 and S4 and S6, respectively (Table 1). Arsenic and Pb concentrations decreased much more rapidly between S4 and S5 (Table 1), suggesting that mobilised Sb may be transported over longer distances than both As and Pb before being attenuated by the gully soils. Mitsunobu *et al.* (2006) found that, where Sb and As behaved differently in soil, Sb was almost exclusively present in its oxidised form (Sb^V) whilst As was present as a mixture of As^{III} and As^V, indicative of the greater stability of Sb^V in soil–water systems. In addition to its stability in the soil porewaters (Mitsunobu *et al.*, 2006), Sb^V sorbs less strongly to Fe oxides than As^V over a wide pH range (Leuz *et al.*, 2006). In this study, there was a distinct change in solid phase associations of As with distance down-gully. The

sequential extraction data for S5 soils showed that, in contrast with Sb, the majority of solid phase As was associated with Fe oxides and with organic matter, which may also be intimately associated with Fe oxides. Moreover, the porewater profile of As was very similar to that of Fe, the majority of this As was in the colloidal fraction and, from the gel electrophoresis, As was mainly associated with large Fe-rich organic colloids. Although Sb was also associated with the same type of colloids, a greater proportion was present in truly dissolved forms. Thus the extent of sorption to Fe oxides may at least in part explain the observed trends with distance down-gully from SpH1.

Fig. 5. Distribution of Sb, As, Pb and Fe across gel electrophoretic fractions obtained for the colloid fraction (3 kDa–0.2 μm) isolated from S5 porewaters.

4.2.2. Down-gully from SpH1

There were ~2-fold and ~9-fold decreases in the maximum Sb concentration in the solid phase soils between S4 and S5 and S4 and S6, respectively (Table 1). Arsenic and Pb concentrations decreased much more rapidly between S4 and S5 (Table 1), suggesting that mobilised Sb may be transported

over longer distances than both As and Pb before being attenuated by the gully soils. Mitsunobu *et al.* (2006) found that, where Sb and As behaved differently in soil, Sb was almost exclusively present in its oxidised form (Sb^V) whilst As was present as a mixture of As^{III} and As^V, indicative of the greater stability of Sb^V in soil–water systems. In addition to its stability in the soil porewaters (Mitsunobu *et al.*, 2006), Sb^V sorbs less strongly to Fe oxides than As^V over a wide pH range (Leuz *et al.*, 2006). In this study, there was a distinct change in solid phase associations of As with distance down-gully. The sequential extraction data for S5 soils showed that, in contrast with Sb, the majority of solid phase As was associated with Fe oxides and with organic matter, which may also be intimately associated with Fe oxides. Moreover, the porewater profile of As was very similar to that of Fe, the majority of this As was in the colloidal fraction and, from the gel electrophoresis, As was mainly associated with large Fe-rich organic colloids. Although Sb was also associated with the same type of colloids, a greater proportion was present in truly dissolved forms. Thus the extent of sorption to Fe oxides may at least in part explain the observed trends with distance down-gully from SpH1.

As for the results for S3 soils, sequential extraction data for 4–6 cm samples from both S4 and S5 revealed that ~80% Sb was present in the residual phase. At 8–10 cm in S4, there was a decrease in association with organic matter and the percentage in the residual phase had increased to >90%. The distributions of As and Pb were similar to that of Sb at both 4–6 cm and 8–10 cm in S4, which suggests a very low potential for remobilisation of all three elements at this location. At S5, however, because As was almost evenly distributed amongst the iron oxide, organic matter and residual phases and could thus be more susceptible to redox-related remobilisation and loss from the soils should prevailing conditions change in the future.

The Sb concentrations in the porewaters at S4 were ~2–4 times greater than at S3, whilst the S4 solid phase concentrations were only slightly higher than those at S3. Since the sequential extraction data showed very little difference in the solid phase associations of Sb, and the pH of the S4 soils (~4.7–4.9) was similar to that of the surface spoil (~4.8), the higher S4 porewater Sb concentrations are attributed to rainwater-induced leaching from the spoil, which was ~5 m upslope (cf Filella *et al.*, 2009; Biver and Shotyk, 2013). Moreover, the much higher solid phase Pb concentrations at S4 in comparison with S3 were not reflected in higher porewater concentrations, suggesting a lower leachability of Pb from the spoil in comparison with Sb. This is consistent with the data for the spoil which, as discussed above, indicated preferential loss of Sb (and As) from SpH1-surface samples (Table 1). In the S4 porewaters, both Sb and As were predominantly present in truly dissolved form. The small amount of Sb present in colloidal forms was associated with smaller organic colloids which had a low Fe content. In contrast, the small amount of colloidal As at S4 was mainly associated with larger Fe-rich colloids, providing an additional explanation for its more rapid removal to the solid phase during its down-gully transport.

Comparing S4 and S5 porewaters, the maximum Sb concentration decreased by a factor of ~2 whilst that of As decreased by ~10. Thus for Sb and As, this trend mirrored that described above for the solid phase, providing further support for the poorer attenuation of Sb by the gully soils. One potential anomaly, however, was that the distributions of Pb and As at S5 were similar and, although the solid phase Pb concentration had decreased by a factor of ~15, porewater Pb concentrations were similar to those at S4. In the porewaters of both S4 and S5, Pb, Fe and DOM (colour retention) were almost exclusively found in the colloidal fraction whilst >~50% Sb and ≤70% As was present in the truly dissolved fraction. Gel electrophoretic fractionation of the colloid fraction of porewaters from the 4–6 cm section of S5 then revealed further important differences in elemental speciation. Antimony and As present within the colloidal fraction were both associated with large Fe rich organic colloids whilst Pb was associated with smaller organic colloids which contained low concentrations of iron (Fig. 5). In agreement with Graham *et al.* (2011) and Crançon et al. (2010), who showed that association with small Fe-poor organic colloids inhibited the removal of depleted uranium (DU) from firing range soils, small organic-colloidal association of Pb inhibits its removal from the porewaters to the solid phase of the S5 gully soils. Fig.5. Distribution of Sb, As, Pb and Fe across gel electrophoretic fractions obtained for the colloid fraction (3 kDa–0.2 μm) isolated from S5 porewaters.

4.3. Impact upon receiving waters

The Sb concentrations of ~6–8 μg L^{-1} and ~84 μg L^{-1} for W3 (downstream of gully) and W4 (surface flow closest to SpH1), respectively, were in reasonable agreement with those previously reported for downstream (14.3 μg L^{-1}) and spoil heap drainage (60.4 μg L^{-1}) samples (Mohammad *et al.,* 1990). The Sb concentrations at W3 were more than an order of magnitude higher than the value of 0.11 μg L^{-1} in the upstream waters (W1–2). The latter was in line with those published in an extensive review by Filella *et al.* (2002b) where concentrations ranged from 0.17 μg L−1 in pristine water at Loch Ewe, Scotland, to 1.9 μg L^{-1} in the urbanised River Trent (Apte and Howard, 1986; Filella *et al*., 2002b; Jarvie et al., 2000). For As, water concentrations can be more variable due to local mineralogy, with natural concentrations ranging between 1 and 10 μg L−1 (Jarvie *et al.,* 2000). The values of ~1–1.1 μg L^{-1} for W1–2 fell within this range whilst that for W3 (~13–20 μg L^{-1}) only slightly exceeded the natural concentration range and was much lower than concentrations of ≤283 μg L^{-1} found downstream of an abandoned Slovakian Sb mine (Hiller *et al.*, 2012). Nevertheless, the water from W4 and W5 exceeded the 50.0 μg L^{-1} As freshwater Environmental Quality Standard (EQS) (SEPA, 2013).

5. Conclusions

In the vicinity of the small spoil heap, SpH2, at Glendinning, Scotland, Sb, As, Pb and Fe are released into soil porewaters as a consequence of DOM production and leaching. The extent of colloid association and indeed the speciation within the colloid fraction varied for each element. Importantly, Sb was mainly present in truly dissolved forms towards the bottom of the soil profiles whilst greater proportions of As, Pb and Fe were present in the colloidal fraction. The decreasing solid phase Sb concentrations with depth were therefore a consequence of the loss of truly dissolved Sb from the deepest sections of the soil profiles. The movement of rainwater through the main spoil heap, SpH1, mobilised Sb and As, which were then transported down a steep gully via soil porewaters and surface flows to the Glenshanna Burn. Arsenic was more rapidly removed from the porewaters to the solid phase as a consequence of its stronger associations with Fe oxides. There were clear trends of decreasing solid phase concentrations of Sb, As and Pb with distance down-gully, demonstrating a degree of natural attenuation for all three elements even in steeply sloping organic-rich parts of the catchment. The transport of Sb and As from mineral-rich spoil to the Glenshanna Burn demonstrates mobility in the surrounding area. Although the Glendinning Sb mine has been closed for approximately a century, its environmental impact has left a legacy in the surrounding area, and whilst the Glenshanna Burn complies with the current EQS values, this may not be the case in the future, especially if environmental change leads to increasingly stormy conditions.

Appendix A. Supplementary data

Supplementary data to this article can be found online at
http://dx.doi.org/10.1016/j.scitotenv.2015.04.039.

References

Ackerman, S., Giere, R., Newville, M., Majzlan, J., 2009. Antimony sinks in the weathering crust of bullets from Swiss shooting ranges. Sci. Total Environ. 407, 1669–1682.

Apte, S.C., Howard, A.G., 1986. Determination of dissolved inorganic antimony (V) and antimony (III) species in natural waters by hydride generation atomic absorption spectrometry. J. Anal. At. Spectrom. 1, 221–225.

Bach, C., Dauchy, X., Chagnon, M.-C., Etienne, S., 2012. Chemical compounds and toxicological assessments of drinking water stored in polyethylene terephthalate (PET) bottles: a source of controversy reviewed. Water Res. 46, 571–583.

Biver, M., Shotyk, W., 2012. Stibnite (Sb_2S_3) oxidative dissolution kinetics from pH 1 to 11. Geochim. Cosmochim. Acta 79, 127–139.

Biver, M., Shotyk, W., 2013. Stibiconite (Sb_3O_6OH), senarmontite (Sb_2O_3) and valentinite (Sb_2O_3): dissolution rates at pH 2–11 and isoelectric points. Geochim. Cosmochim. Acta 109, 268–279.

Buschmann, J., Sigg, L., 2004. Antimony(III) binding to humic substances: influence of pH and type of humic acid. Environ. Sci. Technol. 38, 4535–4541.

Buschmann, J., Kappeler, A., Lindauer, U., Kistler, D., Berg, M., Sigg, L., 2006. Arsenite and arsenate binding to dissolved humic acids: influence of pH, type of humic acid and aluminum. Environ. Sci. Technol. 40, 6015–6020.

Butterman, W.C., Carlin, J.F., 2004. Mineral Commodity Profiles—Antimony. U.S. Department of the Interior, U.S. Geological Survey (Open-file report 03-019).

Ceriotti, G., Amarasiriwardena, D., 2009. A study of antimony complexed to soil-derived humic acids and inorganic antimony species along a Massachusetts highway. Microchem. J. 91, 85–93.

Cloy, J.M., Farmer, J.G., Graham, M.C., MacKenzie, A.B., 2009. Retention of As and Sb in ombrotrophic peat bogs: records of As, Sb, and Pb deposition at four Scottish sites. Environ. Sci. Technol. 43, 1756–1762.

Crançon, P., Pili, E., Charlet, L., 2010. Uranium facilitated transport by water-dispersible colloids in field and soil columns. Sci. Total Environ. 408, 2118–2128.

Davidson, C.M., Duncan, A.L., Littlejohn, D., Ure, A.M., Garden, L.M., 1998. A critical evaluation of the three-stage BCR sequential extraction procedure to assess the potential mobility and toxicity of heavy metals in industrially-contaminated land. Anal. Chim. Acta 363, 45–55.

European Commission, 2000. Directive 2000/60/EC of the European Parliament and of the Council of 23 October 2000 Establishing a Framework for Community Action in the Field of Water Policy (Water Framework Directive). European Commission. European Commission, 2001. Directive 76/464/EEC Article 7 of the European Parliament and of the Council on Pollution Reduction Programmes (Water Framework Directive). European Commission.

Farmer, J.G., Eades, L.J., Graham, M.C., Cloy, J.M., Bacon, J.R., 2010. A comparison of the isotopic composition of lead in rainwater, surface vegetation and tree bark at the long term monitoring site, Glensaugh, Scotland, in 2007. Sci. Total Environ. 408, 3704–3710.

Filella, M., 2011. Antimony interactions with heterogeneous complexants in waters, sediments and soils: a review of data obtained in bulk samples. Earth Sci. Rev. 107, 325–341.

Filella, M., Belzile, N., Chen, Y.-W., 2002a. Antimony in the environment: a review focused on natural waters: I. Occurrence. Earth Sci. Rev. 57, 125–176.

Filella, M., Belzile, N., Chen, Y.-W., 2002b. Antimony in the environment: a review focused on natural waters: II. Relevant solution chemistry. Earth Sci. Rev. 59, 265–285.

Filella, M., Philippo, S., Belzile, N., Chen, Y., Quentel, F., 2009. Natural attenuation processes applying to antimony: a study in the abandoned antimony mine in Goesdorf, Luxembourg. Sci. Total Environ. 407, 6205–6216.

Flynn, H.C., Meharg, A.A., Bowyer, P.K., Paton, G.I., 2003. Antimony bioavailability in mine soils. Environ. Pollut. 124, 93–100.

Gál, J., Hursthouse, A., Cuthbert, S., 2007. Bioavailability of arsenic and antimony in soils from an abandoned mining area, Glendinning (SW Scotland). J. Environ. Sci. Health A 42, 1263–1274.

Gallagher, M.J., Stone, P., Kemp, A.E.S., Hills, M.G., Jones, R.C., Smith, R.T., Peachey, D., Vickers, B.P., Parker, M.E., Rollin, K.E., Skilton, B.R.H., 1983. Strata bound arsenic and vein antimony mineralisation in Silurian greywackes at Glendinning, South Scotland. Institute of Geological Sciences Mineral Reconnaissance Programme (Report no. 59).

Graham, M.C., Vinogradoff, S.I., Chipchase, A.J., Dunn, S.M., Bacon, J.R., Farmer, J.G., 2006. Using size fractionation and Pb isotopes to study Pb transport in organic-rich upland catchments, NE Scotland. Environ. Sci. Technol. 40, 1250–1256.

Graham, M.C., Oliver, I.W., MacKenzie, A.B., Ellam, R.M., Farmer, J.G., 2008. An integrated colloid fractionation approach applied to the characterisation of porewater uranium–humic interactions at a depleted uranium contaminated site. Sci. Total Environ. 404, 207–217.

Graham, M.C., Oliver, I.W., MacKenzie, A.B., Ellam, R.M., Farmer, J.G., 2011. Mechanisms controlling lateral and vertical porewater migration of depleted uranium (DU) at two UK weapons testing sites. Sci. Total Environ. 409, 1854–1866.

He, M., Wang, X., Wu, F., Fu, Z., 2012. Antimony pollution in China. Sci. Total Environ. 421–422, 41–50.

Hiller, E., Lalinská, B., Chovan, M., Jurkovič, Ľ., Klimko, T., Jankulár, M., Hovorič, R., Šottník, P., Fľaková, R., Ženišová, Z., Ondrejková, I., 2012. Arsenic and antimony contamination of waters, stream sediments and soils in the vicinity of abandoned antimony mines in the Western Carpathians, Slovakia. Appl. Geochem. 27, 598–614.

International Agency for Research on Cancer (IARC), 1989. IARC Monograph vol. 47. World Health Organisation, Lyon, France, p. 291 ISBN 92 83212479; ISSN 02509555.

Jarvie, H.P., Neal, C., Burton, J.D., Tappin, A.D., 2000. Patterns in trace element chemistry in the freshwater tidal reaches of the River Trent. Sci. Total Environ. 251/252, 317–333.

Johnson, C.A., Moench, H., Wersin, P., Kugler, P., Wenger, C., 2005. Solubility of antimony and other elements in samples taken from shooting ranges. J. Environ. Qual. 34, 248–254.

Kalbitz, K., Solinger, S., Park, J.-H., Michalzik, B., Matzner, E., 2000. Controls on the dynamics of dissolved organic matter in soils: a review. Soil Sci. 165, 277–304.

Kalbitz, K., Kaiser, K., 2008. Contribution of dissolved organic matter to carbon storage in forest mineral soils. J. Plant Nutr. Soil Sci. 171, 52–60.

Leuz, A.-K., Mönch, H., Johnson, C.A., 2006. Sorption of Sb(III) and Sb(V) to goethite: influence on Sb(III) oxidation and mobilization. Environ. Sci. Technol. 40, 7277–7282.

Michazik, B., Matzner, E., 1999. Dynamics of dissolved organic nitrogen and carbon in a Central European Norway spruce ecosystem. Eur. J. Soil Sci. 50, 579–590.

Mitsunobu, S., Harada, T., Takahashi, Y., 2006. Comparison of antimony behaviour with that of arsenic under various soil redox conditions. Environ. Sci. Technol. 40, 7270–7276.

Mitsunobu, S., Takahashi, Y., Terada, Y., Sakata, M., 2010. Antimony(V) incorporation into synthetic ferrihydrite, goethite, and natural iron oxyhydroxides. Environ. Sci. Technol. 44, 3712–3718.

Mohammad, B., Ure, A.M., Reglinski, J., Littlejohn, D., 1990. Speciation of antimony in natural waters: the determination of Sb (III) and Sb (V) by continuous flow hydride generation–atomic absorption spectrometry. Chem. Speciat. Bioavailab. 3, 117–122.

Neubauer, E., Kohler, S.J., Laudon, H., von der Kammer, F., Hofmann, T., 2013. Effect of pH and stream order on iron and arsenic speciation in boreal catchments. Environ. Sci. Technol. 47, 7120–7128.

Okkenhaug, G., Zhu, Y.-G., Luo, L., Lei, M., Li, X., Mulder, J., 2011. Distribution, speciation and availability of antimony (Sb) in soils and terrestrial plants from an active Sb mining area. Environ. Pollut. 159, 2427–2434.

Redman, A.D., Macalady, D.L., Ahmann, D., 2002. Natural organic matter affects arsenic speciation and sorption onto hematite. Environ. Sci. Technol. 36, 2889–2896.

Salminen, R. (chief Ed.), Batista, M.J., Bidovec, M., Demetriades, A., De Vivo, B., De Vos, W. *et al.,* 2005. Geochemical Atlas of Europe. Part 1 — Background Information, Methodology and Maps. Geological Survey of Finland, Otamedia Oy, Espoo, 525 pp.

Schroth, A.W., Bostick, B.C., Kaste, J.M., Friedland, A.J., 2008. Lead sequestration and species redistribution during soil organic matter decomposition. Environ. Sci. Technol. 42, 3627–3633.

SEPA, Scottish Environment Protection Agency, 2013. Supporting Guidance (WAT-SG-53)—Environmental Standards for Discharges to Surface Waters. Ver: 4.0.

Shi, Z., Allen, H.E., Di Toro, D.M., Lee, S.-Z., Harsh, J.B., 2013. Predicting Pb^{II} adsorption on soils: the roles of soil organic matter, cation competition and iron (hydr)oxides. Environ. Chem. 10, 465–474.

Steely, S., Amarasiriwardena, D., Xing, B., 2007. An investigation of inorganic antimony species and antimony associated with soil humic acid molar mass fractions in contaminated soils. Environ. Pollut. 148, 590–598.

Taylor, S.R., 1964. Abundance of chemical elements in the continental crust: a new table. Geochim. Cosmochim. Acta 28, 1273–1285.

U.S. Geological Survey, 2013. Mineral Commodity Summaries 2013. U.S. Geological Survey, p. 198.

Walker, F.P., Schreiber, M.E., Rimstidt, J.D., 2006. Kinetics of arsenopyrite oxidative dissolution by oxygen. Geochim. Cosmochim. Acta 70, 1668–1676.

Wedepohl, K.H., 1995. The composition of the continental crust. Geochim. Cosmochim. Acta 59, 1217–1232.

Wilson, S.C., Lockwood, P.V., Ashley, P.M., Tighe, M., 2010. The chemistry and behaviour of antimony in the soil environment with comparisons to arsenic: a critical review. Environ. Pollut. 158, 1169–1181.

Yafa, C., Farmer, J.G., 2006. A comparative study of acid-extractable and total digestion methods for the determination of inorganic elements in peat material by inductively coupled plasma-optical emission spectrometry. Anal. Chim. Acta 557, 296–303.

Yafa, C., Farmer, J.G., Graham, M.C., Bacon, J.R., Barbante, C., Cairns, W.R.L., Bindler, R., Renberg, I., Cheburkin, A., Emons, H., Handley, M.J., Norton, S.A., Krachler, M., Shotyk, W., Li, X.D., Martinez-Cortizas, A., Pulford, I.D., MacIver, V., Schweyer, J., Steinnes, E., SjØbakk, T.E., Weiss, D., Dolgopolova, A., Kylander, M., 2004. Development of an ombrotrophic peat bog (low ash) reference material for the determination of elemental concentrations. J. Environ. Monit. 6, 493–501.